Journal of Power Sources 186 (2009) 224–227

Contents lists available at ScienceDirect

Journal of Power Sources

journal homepage: www.elsevier.com/locate/jpowsour

Short communication

Electrochemical profile of an asymmetric supercapacitor using carbon-coated $LiTi_2(PO_4)_3$ and active carbon electrodes

Jia-Yan Luo, Yong-Yao Xia*

Department of Chemistry & Shanghai Key Laboratory of Molecular Catalysis and Innovative Materials, Fudan University, Shanghai 200433, PR China

ARTICLE INFO

Article history:
Received 14 July 2008
Received in revised form 9 September 2008
Accepted 9 September 2008
Available online 26 September 2008

Keywords:
Aqueous
Electrochemical capacitor
Li_2SO_4
Hybrid
Battery
Energy

ABSTRACT

In this work, we reported an asymmetric supercapacitor in which active carbon (AC) was used as a positive electrode and carbon-coated $LiTi_2(PO_4)_3$ as a negative electrode in 1 M Li_2SO_4 aqueous electrolyte. The $LiTi_2(PO_4)_3$/AC hybrid supercapacitor showed a sloping voltage profile from 0.3 to 1.5 V, at an average voltage near 0.9 V, and delivered a capacity of 30 mAh g^{-1} and an energy density of 27 Wh kg^{-1} based on the total weight of the active electrode materials. It exhibited a desirable profile and maintained over 85% of its initial energy density after 1000 cycles. The hybrid supercapacitor also exhibited an excellent rate capability, even at a power density of 1000 W kg^{-1}, it had a specific energy 15 Wh kg^{-1} compared with 24 Wh kg^{-1} at the power density about 200 W kg^{-1}.

1. Introduction

Supercapacitors coupled with batteries and fuel cells are considered promising mid-term and long-term for low- and zero-emission transport vehicles by providing the power peaks for start-stop, acceleration, and recovering the braking energy. Today much research in electrochemical capacitors aims to increase power and energy density as well as reduce fabrication cost while using environmental friendly materials [1–5]. One of the most useful approaches is to develop a hybrid system that typically consists of an electrochemical double-layer capacitor (EDLC) electrode and a battery electrode, such as AC/$Ni(OH)_2$, AC/MnO_2 and AC/$LiMn_2O_4$ systems [6–8]. Both the increase of the working voltage and the high energy density of the battery electrode material results in a significant increase in the overall energy density of the capacitors compared with that of AC/AC system. It should be noted that, in the above aqueous hybrid supercapacitor systems, the negative electrode materials are all activated carbon, which is characterized by a high hydrogen evolution overpotential that enables a large negative cutoff potential [9,10]. However, there are no appropriate negative materials for supercapacitor to replace AC except RuO_2 until now, but the high cost detracts its application.

Recently, we have demonstrated that the carbon-coated $LiTi_2(PO_4)_3$ exhibited excellent electrochemical performance both in organic and aqueous electrolytes, and especially shown good cycling stability in aqueous electrolytes [11]. $LiTi_2(PO_4)_3$ appears to be a promising material for the novel hybrid supercapacitor negative electrode, because of the appropriate voltage plateau at 2.5 V vs. Li/Li^+ (−0.5 V vs. SHE), high theoretical specific capacity of 138 mAh g^{-1}, low cost of the raw material, and environmentally benign [12–14]. In the present work, the hybrid supercapacitor consisting of a combination of AC as cathode material, carbon-coated $LiTi_2(PO_4)_3$ as anode material, and a 1 M Li_2SO_4 aqueous solution as electrolyte was presented, and the electrochemical performance of the $LiTi_2(PO_4)_3$/AC hybrid supercapacitor was extensively investigated by cyclic voltammentry (CV), and galvanostatic charge–discharge tests.

2. Experiment

Carbon-coated $LiTi_2(PO_4)_3$: the macroporous $LiTi_2(PO_4)_3$ was prepared by a sol–gel method [11]. An aqueous precursor containing Li_2CO_3, $NH_4H_2PO_4$, and TiO_2 was blended with 100 ml of 2 wt.% poly-vinyl-alcohol (PVA) aqueous solution as a synthetic agent. The mixture was stirred at a constant temperature of 80 °C until water has evaporated and a white solid formed. The product was placed in a porcelain boat and heated at 900 °C for 12 h under N_2 flow in a tube furnace. Then the as-prepared $LiTi_2(PO_4)_3$ powder was transferred into a reaction tube to make a fluid-bed layer for reaction where

* Corresponding author. Fax: +86 21 55664177.
E-mail address: yyxia@fudan.edu.cn (Y.-Y. Xia).

0378-7753/$ – see front matter © 2008 Published by Elsevier B.V.
doi:10.1016/j.jpowsour.2008.09.063

a toluene vapor was carried by N_2 through the reaction tube at a flow rate of 1 l min^{-1}. The reaction temperature was maintained at 800 °C for 12 h to coat the surface of $LiTi_2(PO_4)_3$ with a carbon layer about 20 nm. The carbon content of the carbon-coated $LiTi_2(PO_4)_3$ sample is about 12 wt.% by TG analysis (including both the carbon resident in the as-prepared nanostructured $LiTi_2(PO_4)_3$ and CVD coated carbon) and the carbon has been transformed to graphite to a certain extend. The particle size of the carbon-coated $LiTi_2(PO_4)_3$ is in the range of 200–300 nm. BET surface area measurement of the carbon-coated $LiTi_2(PO_4)_3$ yields a value of 0.7 $m^2\ g^{-1}$. The AC was used as received (provided by Research Institute of Chemical Defense, Beijing, China) and had a BET surface area of 1500 $m^2\ g^{-1}$.

The electrodes were formed by mixing 85 wt.% active material, 10 wt.% acetylene black and 5 wt.% PTFE as binder before pressing into a thin sheet of uniform thickness onto stainless steel grid (1.2×10^7 Pa) that served as a current collector (area is 1 cm^2). The typical mass load of positive (AC) and negative (carbon-coated $LiTi_2(PO_4)_3$) electrode material was 14 and 8 mg, respectively. The electrolyte was 1 M Li_2SO_4 solution. The electrochemical behavior of the individual composite electrode was characterized by cyclic voltammetry (CV). The experiments were carried out in a three-electrode glass cell. Platinum foil was used as a counter electrode, and saturated calomel electrode (SCE, 0.242 V vs. NHE) as the reference electrode. Cyclic voltammetry test was performed using a Solartron Instrument Model 1287 electrochemical interface controlled by a computer. Capacitor test was using a two-electrode glass cell, it was consisted of a AC positive electrode and $LiTi_2(PO_4)_3$ negative electrode.

3. Results and discussion

Fig. 1 shows the cyclic voltammograms (CV) of carbon-coated $LiTi_2(PO_4)_3$ and AC electrodes. The CV of the carbon-coated $LiTi_2(PO_4)_3$ electrode in aqueous 1 M Li_2SO_4 solution (Fig. 1a) is characterized by a set of oxidation and reduction peaks centered at −0.6 and −0.9 V (potential vs. SCE), respectively, which are in good agreement with the extraction/insertion reaction of $LiTi_2(PO_4)_3$ in the organic electrolyte. The hydrogen evolution reaction (HER) on the $LiTi_2(PO_4)_3$ electrode occurs under −1.0 V (potential vs. SCE), indicating that the Li^+ can be inserted into the $LiTi_2(PO_4)_3$ lattice before the evolution of H_2. It should be noted that the carbon coating is needed to improve the stability of in aqueous electrolyte. The uncoated $LiTi_2(PO_4)_3$ shows fast capacity fading in aqueous electrolyte, which is extensively found for the electrode materials with potentials lower than 3.0 V vs. Li/Li^{i+} in aqueous electrolyte. It has been suggested that the capacity fading is related to transition metal ion dissolution, phase transformation of electrode materials, decomposition of water, and so on [15]. We speculate that the capacity fading mechanism of $LiTi_2(PO_4)_3$ is most likely ascribed to changes in the composition and/or phase structure because of a side reaction with water in the aqueous electrolyte. So we employed a surface carbon-coated technique to improve the stability of electrode material by preventing water from attacking the bulk phase [11]. However, the lithium insertion into the carbon generally takes place at potentials lower than 1.5 V vs. Li/Li^+, the lithium ion intercalates $LiTi_2(PO_4)_3$ at 2.5 V vs. Li/Li^+. It is seem that the carbon coated by CVD process spreads over the entire particle surface to form a nanometer-thick film will prevent the lithium ion from intercalating $LiTi_2(PO_4)_3$. Presently, the mechanism responsible for ionic transport in the coatings still remains unclear. Recently, Suzuki reported that the lithium ion can diffuse through a copper thin film [16]. This was further confirmed by an *ab initio* density-functional calculation contributed by Chen and co-workers [17]. They demonstrated that the ion can pass through the film by some crystal defect

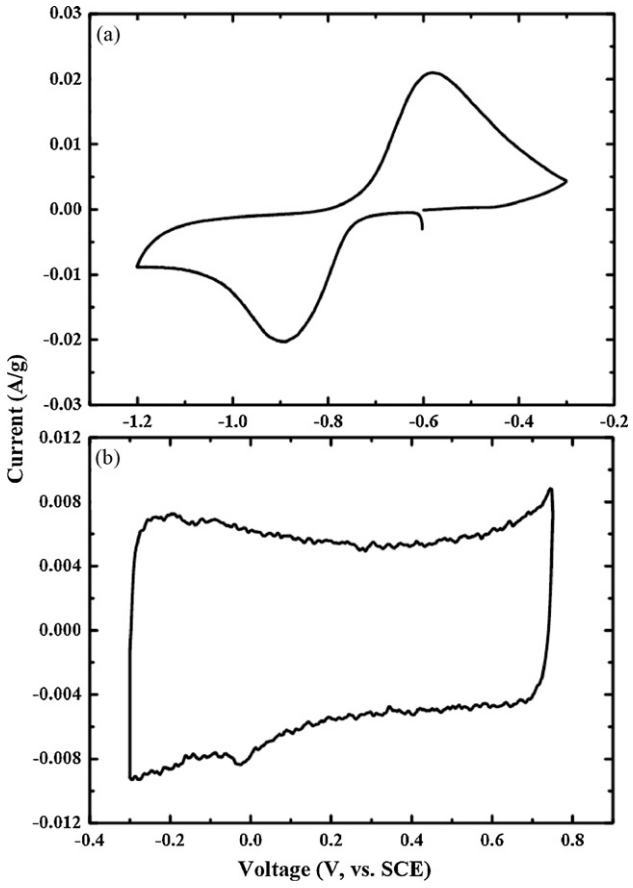

Fig. 1. CV curves of (a) carbon-coated $LiTi_2(PO_4)_3$ sample, and (b) AC sample at a scan rate of 3 mV s^{-1}.

or vacancy in the bulk substance under the ion concentration in between two phase. There are many defects present in our coated-carbon layer. It is speculated that these defects allow the Li ion to pass through the carbon layer to provide enough effective reaction areas. The AC electrode (Fig. 1b) can be cycled between −0.3 and 0.75 V (potential vs. SCE) without noticeable oxygen evolution. Within this potential window, the shape of the CV is rectangular as expected for material displaying capacitive behavior.

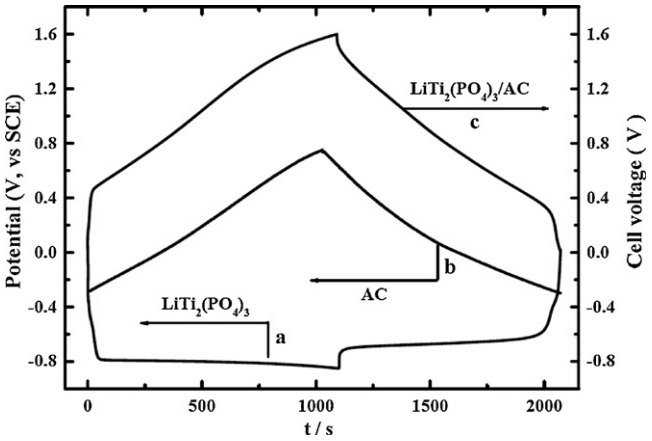

Fig. 2. Typical charge/discharge curves of individual electrode (a) carbon-coated $LiTi_2(PO_4)_3$ and (b) AC along with (c) a composite voltage profile of the $LiTi_2(PO_4)_3$/AC hybrid aqueous capacitor at a current rate of 2 mA cm^{-2} in 1 M Li_2SO_4.

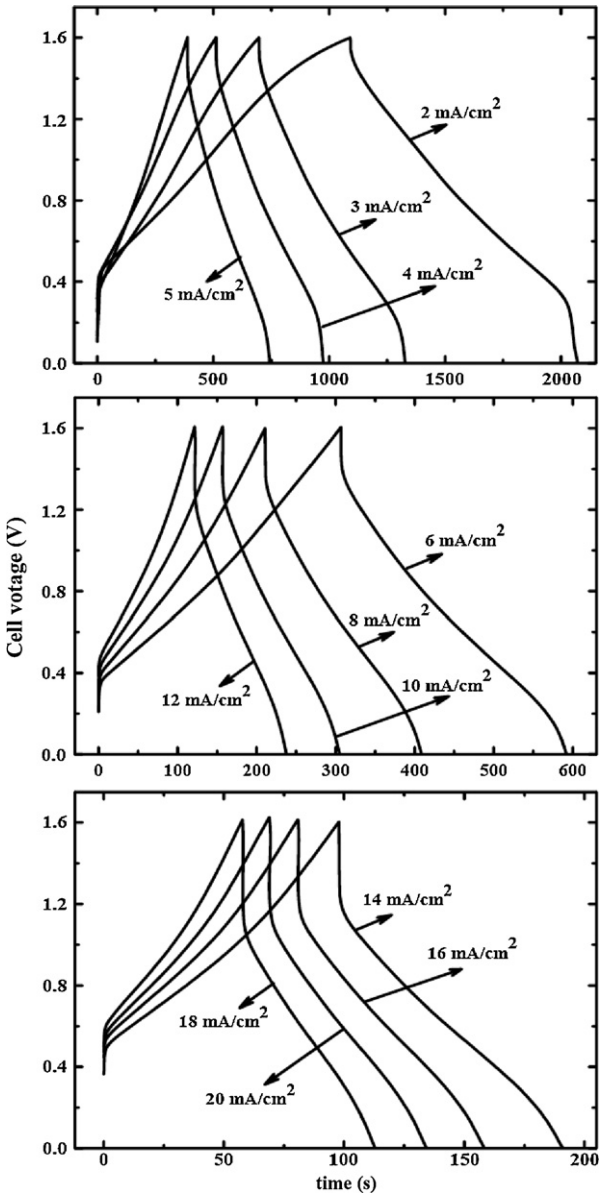

Fig. 3. Galvanostatic charge/discharge curves of the $LiTi_2(PO_4)_3$/AC hybrid aqueous capacitor in 1 M Li_2SO_4 between 0 and 1.6 V at various current rates from 2 to 20 mA cm^{-2}.

Fig. 2 shows the charge/discharge curves of individual carbon-coated $LiTi_2(PO_4)_3$ and AC electrode along with a composite voltage profile of the $LiTi_2(PO_4)_3$/AC hybrid aqueous cell at a current rate of 2 mA cm^{-2} in 1 M Li_2SO_4. Considering the safe potentials of both electrodes without O_2 and H_2 evolution, the cutoff potentials for $LiTi_2(PO_4)_3$ and AC were set at −0.85 and 0.75 V vs. SCE, respectively. This corresponds to a delivered capacity of about 90 mAh g^{-1} (excluding the carbon content about 12 wt.%) for $LiTi_2(PO_4)_3$ and 45 mAh g^{-1} for the AC electrode. In other words, this gives the charge cutoff voltage of the cell at 1.6 V by controlling the positive/negative electrode mass ratio load of 2:1, as shown in Fig. 2c. The cell shows a sloping voltage profile from 0.3 to 1.5 V, at an average voltage near 0.9 V, and delivers a capacity of 30 mAh g^{-1} based on the total weight of the active electrode materials.

Fig. 3 shows the galvanostatic charge/discharge curves of the carbon-coated $LiTi_2(PO_4)_3$/AC hybrid aqueous cell with a mass ratio of 2:1 in 1 M Li_2SO_4 between 0 and 1.6 V at various current rates from 2 to 20 mA cm^{-2}. The curves are almost linear and the sudden drop of potential at the beginning of charge and discharge is associated to the ohmic resistance of the cell. The average internal resistance of the capacitor can be calculated according to $R = (V_{charge} - V_{discharge})/(2I)$, where V_{charge} and $V_{discharge}$ are, respectively, the cell voltage at the end of charge and at the beginning of the discharge, and I is absolute value of the current which is the same during the charge and the discharge. This gives an average value of 21 Ω, reflecting the non-optimized electric contacts between the active electrode materials and the current collectors, the solution resistance. The capacitance calculated from the discharge curves decreases from 28 mAh g^{-1} at 3 mA cm^{-2} to 16 mAh g^{-1} at 20 mA cm^{-2}, suggesting that the capacitor presents excellent rate capability.

The Ragone plots of Fig. 4 summarize the performance of the capacitor tested under various charge/discharge currents between 1.6 and 0 V relative to Fig. 3. The specific power density (P) and energy density (E) of the hybrid supercapacitor are calculated as follows

$$P = \Delta E \times \frac{I}{m}$$

$$E = P \times t$$

$$\Delta E = \frac{E_{max} + E_{min}}{2}$$

where E_{max} and E_{min} are, respectively, the potential at the beginning of discharge and at the end of discharge, I is the charge/discharge current, t is the discharge time, and m is the mass of active materials including both the positive and negative electrode in the hybrid supercapacitor. The specific energy and power density of the hybrid supercapacitor shown in Fig. 4 are calculated by using the total weight of the active electrode materials, the cell voltage, and the capacity based on the charge/discharge curves shown in Fig. 3. The data of Fig. 4 clearly demonstrates that the $LiTi_2(PO_4)_3$/AC hybrid supercapacitor has a good specific energy and power density. For example, the specific energy is 24 Wh kg^{-1} at a power density of about 200 W kg^{-1} and still keeps 15 Wh kg^{-1} at a power density of 1000 W kg^{-1}.

The cycling stability of the $LiTi_2(PO_4)_3$/AC hybrid supercapacitor upon charge/discharge cycling was tested in 1 M Li_2SO_4 between 0 and 1.6 V at a current rate of 10 mA cm^{-2} is illustrated in Fig. 5.

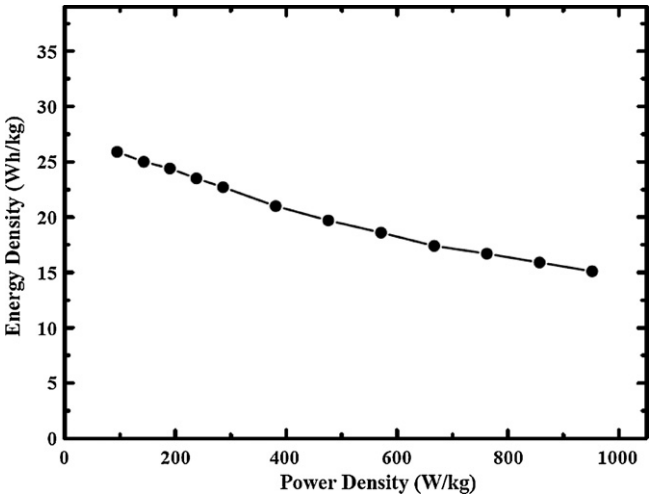

Fig. 4. Ragone plot of the $LiTi_2(PO_4)_3$/AC hybrid aqueous capacitor in 1 M Li_2SO_4 between 0 and 1.6 V. The energy densities and power densities are calculated base on the total weight of the active materials of both electrodes.

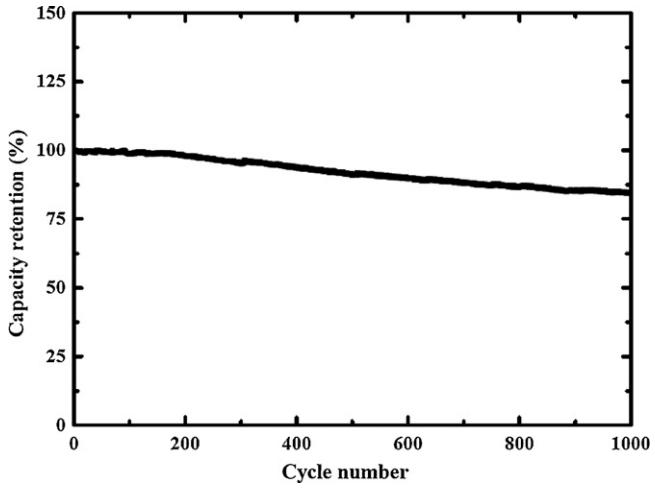

Fig. 5. Cycling life profile of the $LiTi_2(PO_4)_3$/AC hybrid aqueous capacitor in 1 M Li_2SO_4 between 0 and 1.6 V at a current rate of 10 mA cm^{-2}.

The hybrid supercapacitor exhibited a desirable cycle profile and maintained over 85% of its initial energy density after 1000 cycles. The capacitance fading upon cycling is mainly due to the instability of $LiTi_2(PO_4)_3$ in aqueous electrolyte. This agrees well with previous reports about aqueous lithium ion batteries [15]. The mechanism of capacity fading of lithium intercalated compound in aqueous electrolyte is very complicate, and much work should be done in the future. So much better cycling performance would be expected for the $LiTi_2(PO_4)_3$/AC supercapacitors if the stability of $LiTi_2(PO_4)_3$ in aqueous electrolyte is improved.

4. Conclusion

A novel hybrid supercapacitor in which AC is used as a positive electrode and a carbon-coated lithium-ion intercalated compound $LiTi_2(PO_4)_3$ as a negative electrode in 1 M Li_2SO_4 mild aqueous electrolyte has been introduced. The carbon-coated $LiTi_2(PO_4)_3$ and AC, respectively, deliver a capacity of 90 and 45 mAh g^{-1} within safe potentials without O_2 and H_2 evolution, and allow the design of a 1.6 V hybrid supercapacitor by controlling the positive/negative electrode mass ratio load of 2:1. The novel carbon-coated $LiTi_2(PO_4)_3$/AC hybrid supercapacitor shows a sloping voltage profile from 0.3 to 1.5 V, at an average voltage near 0.9 V, and delivers a capacity of 30 mAh g^{-1} and an energy density of 27 Wh kg^{-1} based on the total weight of the active electrode materials. The hybrid supercapacitor maintains 85% of its initial energy density after 1000 cycles. It also exhibits an excellent rate capability.

Acknowledgements

This work was partially supported by the National Natural Science Foundation of China (No. 20633040), the 863 program of China (No. 2006AA05Z218) and the State Key Basic Research Program of PRC (2007CB9700). J. Y. Luo acknowledges the support of Fudan Graduate Innovation Funds.

References

[1] B.E. Conway, Electrochemical Supercapacitors, Scientific Fundamentals and Technological Applications, Kluwer Academic/Plenum Publishers, New York, 1997.
[2] S. Sarangapani, B.V. Tilak, C.P. Chen, J. Electrochem. Soc. 143 (1996) 3791.
[3] B.E. Conway, V. Birss, J. Wojtowicz, J. Power Sources 66 (1997) 1.
[4] B.E. Conway, J. Electrochem. Soc. 138 (1991) 1539.
[5] N. Miura, S. Oonishi, K.R. Prasad, Electrochem. Solid State Lett. 7 (2004) A247.
[6] S.M. Lika, D.E. Reisner, J. Dai, R. Cepulis, Proceedings of the 11th International Seminar on Double Layer Capacitors, Florida Educational Seminars Inc., 2001.
[7] T. Brousse, M. Toupin, D. Bĭelanger, J. Electrochem. Soc. 151 (2004) A614.
[8] Y.G. Wang, J.Y. Luo, C.X. Wang, Y.Y. Xia, J. Electrochem. Soc. 153 (2006) A1425.
[9] S.C. Pang, M.A. Anderson, T.W. Chapman, J. Electrochem. Soc. 147 (2000) 444.
[10] T. Brousse, D. Bĭelanger, Electrochem. Solid State Lett. 6 (2003) A244.
[11] J.Y. Luo, Y.Y. Xia, Adv. Funct. Mater. 17 (2007) 3877.
[12] A. Aatiq, M. Menetrier, L. Croguennee, E. Suard, C. Delma, J. Mater. Chem. 12 (2002) 2971.
[13] S. Patoux, C. Masquelier, Chem. Mater. 14 (2002) 2057.
[14] C.M. Burba, R. Frech, Solid State Ionics 177 (2006) 1489.
[15] W. Li, J.R. Dahn, D. Wainwright, Science 264 (1994) 1115.
[16] J. Suzuki, Y. Yoshida, C. Nakahara, K. Sekine, M. Kikuchi, T. Takamura, Electrochem. Solid State Lett. 4 (2001) A1.
[17] Z. Xiong, S. Shi, C. Ouyang, M. Lei, L. Hu, Y. Ji, Z. Wang, L. Chen, Phys. Lett. A 337 (2006) 247.